

1 **A GENERALISED RANDOM ENCOUNTER MODEL FOR ESTIMATING**
2 **ANIMAL DENSITY WITH REMOTE SENSOR DATA**

3 **Running title: A generalised random encounter model for animals.**

4 **Word count:**

5 **Authors:**

6 Tim C.D. Lucas^{1,2,3}, Elizabeth A. Moorcroft^{1,4,5}, Robin Freeman⁵, Marcus J. Rowcliffe⁵,
7 Kate E. Jones^{2,5}

8 **Addresses:**

9 1 CoMPLEX, University College London, Physics Building, Gower Street, Lon-
10 don, WC1E 6BT, UK

11 2 Centre for Biodiversity and Environment Research, Department of Genetics,
12 Evolution and Environment, University College London, Gower Street, London,
13 WC1E 6BT, UK

14 3 Department of Statistical Science, University College London, Gower Street,
15 London, WC1E 6BT, UK

16 4 Department of Computer Science, University College London, Gower Street,
17 London, WC1E 6BT, UK

18 5 Institute of Zoology, Zoological Society of London, Regents Park, London, NW1
19 4RY, UK

20 **Corresponding authors:**

21 Kate E. Jones,
22 Centre for Biodiversity and Environment Research,
23 Department of Genetics, Evolution and Environment,
24 University College London,
25 Gower Street,
26 London,
27 WC1E 6BT,
28 UK

29 kate.e.jones@ucl.ac.uk

30

31 Marcus J. Rowcliffe,

32 Institute of Zoology,

33 Zoological Society of London,

34 Regents Park,

35 London,

36 NW1 4RY,

37 UK

38 marcus.rowcliffe@ioz.ac.uk

ABSTRACT

39
40 **1:** Wildlife monitoring technology has advanced rapidly and the use of remote
41 sensors such as camera traps, and acoustic detectors is becoming common in both
42 the terrestrial and marine environments. Current methods to estimate abundance
43 or density require individual recognition of animals or knowing the distance of
44 the animal from the sensor, which is often difficult. A method without these re-
45 quirements, the random encounter model (REM), has been successfully applied to
46 estimate animal densities from count data generated from camera traps. However,
47 count data from acoustic detectors do not fit the assumptions of the REM due to
48 the directionality of animal signals.

49 **2:** We developed a generalised REM (gREM), to estimate absolute animal density
50 from count data from both camera traps and acoustic detectors. We derived the
51 gREM for different combinations of sensor detection widths and animal signal
52 widths (a measure of directionality). We tested the accuracy and precision of this
53 model using simulations of different combinations of sensor detection widths and
54 animal signal widths, number of captures, and models of animal movement.

55 **3:** We find that the gREM produces accurate estimates of absolute animal density
56 for all combinations of sensor detection widths and animal signal widths. How-
57 ever, larger sensor detection and animal signal widths were found to be more pre-
58 cise. While the model is accurate for all capture efforts tested, the precision of the
59 estimate increases with the number of captures. We found no effect of different
60 animal movement models tested on the accuracy and precision of the gREM.

61 **4:** We conclude that the gREM provides an effective method to estimate absolute
62 animal densities from remote sensor count data over a range of sensor and animal
63 signal widths. The gREM is applicable for count data obtained in both marine and
64 terrestrial environments, visually or acoustically (e.g., big cats, sharks, birds, bats
65 and cetaceans). As sensors such as camera traps and acoustic detectors become
66 more ubiquitous, the gREM will be increasingly useful for monitoring unmarked
67 animal populations across broad spatial, temporal and taxonomic scales.

Keywords. acoustic detection, camera traps, marine, population monitoring, simulations, terrestrial

INTRODUCTION

Animal population density is one of the fundamental measures needed in ecology and conservation. The density of a population has important implications for a range of issues such as sensitivity to stochastic fluctuations (Richter-Dyn & Goel, 1972; Wright & Hubbell, 1983) and risk of extinction (Purvis *et al.*, 2000). Monitoring animal population changes in response to anthropogenic pressure is becoming increasingly important as humans modify habitats and change climates as never before (Everatt *et al.*, 2014). Sensor technology, such as camera traps (Rowcliffe & Carbone, 2008; Karanth, 1995) and acoustic detectors (O’Farrell & Gannon, 1999; Clark, 1995; Acevedo & Villanueva-Rivera, 2006) are becoming increasingly used to monitor changes in animal populations (Rowcliffe & Carbone, 2008; Kessel *et al.*, 2014), as they are efficient, relatively cheap and non-invasive (Cutler & Swann, 1999), allowing for surveys over large areas and long periods. However, the problem of converting sampled count data to estimates of density remains as efforts must be made to account for detectability of the animals (Anderson, 2001).

Methods do already exist for estimating animal density but these methods often require additional information that may not be available. For example, capture-mark-recapture methods (Karanth, 1995; Trolle & Kéry, 2003; Soisalo & Cavalcanti, 2006; Trolle *et al.*, 2007; Borchers *et al.*, 2014) require recognition of individuals, distance methods (Harris *et al.*, 2013) require an estimation of how far away individuals are from the sensor (Barlow & Taylor, 2005; Marques *et al.*, 2011). The development of the random encounter model (REM) (a modification of a gas model) enabled animal densities to be estimated from unmarked individuals of a known speed, and sensor detection parameters (Rowcliffe *et al.*, 2008). The REM method has been successfully applied to estimate animal densities from camera trap surveys (Manzo *et al.*, 2012; Zero *et al.*, 2013). However, extending the REM method to other types of sensors (for example acoustic detectors) is more problematic, because the original derivation assumes a relatively narrow sensor width (up to $\pi/2$

98 radians) and that the animal is equally detectable irrespective of its heading (Row-
99 cliffe *et al.*, 2008).

100 Whilst these restrictions are not problematic for most camera trap makes (e.g.
101 Reconyx, Cuddeback), the REM could not be used to estimate densities from cam-
102 era traps with a wider sensor width (e.g. canopy monitoring with fish eye lens
103 (Brusa & Bunker, 2014)). Additionally, the REM method would not be useful in
104 estimating densities from acoustic survey data as the acoustic detector angles are
105 often wider than $\pi/2$ radians. Acoustic detectors are designed for a range of di-
106 verse tasks and environments (Kessel *et al.*, 2014), which will naturally lead to a
107 wide range of sensor detection widths and detection distances. In addition to this,
108 calls emitted by many animals are directional (Blumstein *et al.*, 2011) breaking the
109 assumption of the REM method.

110 There has been a sharp rise in interest around passive acoustic detectors in re-
111 cent years, with a 10 fold increase in publications in the decade between 2000 and
112 2010 (Kessel *et al.*, 2014). Acoustic monitoring is being developed to study many
113 aspects of ecology, including the interactions of animals and their environments
114 (Blumstein *et al.*, 2011; Rogers *et al.*, 2013), the presence and relative abundances of
115 species (Marcoux *et al.*, 2011), and biodiversity of an area (Depraetere *et al.*, 2012).

116 Acoustic data suffers from many of the problems associated with data from
117 camera trap surveys in that individuals are often unmarked so capture-mark-
118 recapture methods cannot be used to estimate densities. In some cases the dis-
119 tance between the animal and the sensor is known, for example when an array of
120 sensors and the position of the animal is estimated by triangulation (Lewis *et al.*,
121 2007). In these situations distance-sampling methods can be applied, a method
122 typically used for marine mammals (Rogers *et al.*, 2013). However, in many cases
123 distance estimation is not possible, for example when single sensors are deployed,
124 a situation typical in the majority of terrestrial acoustic surveys (Elphick, 2008;
125 Buckland *et al.*, 2008). In these cases, only relative measures of local abundance can
126 be calculated, and not absolute densities. This means that comparison of popula-
127 tions between species and sites is problematic without assuming equal detectabil-
128 ity (Schmidt, 2003; Hayes, 2000; Walters *et al.*, 2013). Equal detectability is unlikely

129 because of differences in environmental conditions, sensor type, habitat, species
130 biology.

131 In this study we create a generalised REM (gREM), as an extension to the cam-
132 era trap model of (Rowcliffe *et al.*, 2008), to estimate absolute density from count
133 data from acoustic detectors, or camera traps, where the sensor width can vary
134 from 0 to 2π radians, and the signal given from the animal can be directional. We
135 assessed the accuracy and precision of the gREM within a simulated environment,
136 by varying the sensor detection widths, animal signal widths, number of captures
137 and models of animal movement. We use the simulation results to recommend
138 best survey practice for estimating animal densities from remote sensors.

139 METHODS

140 **Analytical Model.** The REM presented by Rowcliffe *et al.* (2008) adapts the gas
141 model to model count data from camera trap surveys. The REM is derived assum-
142 ing a stationary sensor with a detection width less than $\pi/2$ radians. However, in
143 order to apply this approach more generally, and in particular to acoustic detec-
144 tors, we need both to relax the constraint on sensor detection width, and allow
145 for animals with directional signals. Consequently, we derive the gREM for any
146 detection width, θ , between 0 and 2π with a detection distance r giving a circular
147 sector within which animals can be captured (the detection zone)(Figure 1). Ad-
148 ditionally, we model the animal as having an associated signal width α between
149 0 and 2π (Figure 1, see Appendix S1 for a list of symbols). We start deriving the
150 gREM with the simplest situation, the gas model where $\theta = 2\pi$ and $\alpha = 2\pi$.

151 *Gas Model.* Following Yapp (1956), we derive the gas model where sensors can
152 capture animals in any direction and animal's signal is detectable from any direction($\theta =$
153 2π and $\alpha = 2\pi$). We assume that animals are in a homogeneous environment, and
154 move in straight lines of random direction with velocity v . We allow that our sta-
155 tionary sensor can capture animals at a detection distance r and that if an animal
156 moves within this detection zone they are captured with a probability of one, while
157 animals outside the zone are never captured.

158 In order to derive animal density, we need to consider relative velocity from
159 the reference frame of the animals. Conceptually, this requires us to imagine that

all animals are stationary and randomly distributed in space, while the sensor moves with velocity v . If we calculate the area covered by the sensor during the survey period we can estimate the number of animals the sensor should capture. As a circle moving across a plane, the area covered by the sensor per unit time is $2rv$. The number of expected captures, z , for a survey period of t , with an animal density of D is $z = 2rvtD$. To estimate the density, we rearrange to get $D = z/2rvt$.

gREM derivations for different detection and signal widths. Different combinations of θ and α would be expected to occur (e.g., sensors have different detection widths and animals have different signal widths). For different combinations θ and α , the area covered per unit time is no longer given by $2rv$. Instead of the size of the sensor detection zone having a diameter of $2r$, the size changes with the approach angle between the sensor and the animal. For any given signal width and detector width and depending on the angle that the animal approaches the sensor, the width of the area within which an animal can be detected is called the profile, p . The size of the profile (averaged across all approach angles) is defined as the average profile \bar{p} . However, different combinations of θ and α need different equations to calculate \bar{p} .

We have identified the parameter space for the combinations of θ and α for which the derivation of the equations are the same (defined as sub-models in the gREM) (Figure 2). For example, the gas model becomes the simplest gREM sub-model (upper right in Figure 2) and the REM from Rowcliffe *et al.* (2008) is another gREM sub-model where $\theta < \pi/2$ and $\alpha = 2\pi$. We derive one gREM sub-model SE2 as an example below, where $2\pi - \alpha/2 < \theta < 2\pi$, $0 < \alpha < \pi$ (see Appendix S2 for other gREM sub-models).

Example derivation of SE2. In order to calculate \bar{p} , we have to integrate over the focal angle, x_1 (Figure ??). This is the angle taken from the centre line of the sensor. Other focal angles are possible (x_2, x_3, x_4) and are used in other gREM sub-models (see Appendix S2). As the size of the profile depends on the approach angle, we present the derivation across all approach angles. When the sensor is directly approaching the animal $x_1 = \pi/2$.

Starting from $x_1 = \pi/2$ until $\theta/2 + \pi/2 - \alpha/2$, the size of the profile is $2r \sin \alpha/2$ (Figure ??a). During this first interval, the size of α limits the width of the profile. When the animal reaches $x_1 = \theta/2 + \pi/2 - \alpha/2$ (Figure ??b), the size of the profile is $r \sin(\alpha/2) + r \cos(x_1 - \theta/2)$ and the size of θ and α both limit the width of the profile (Figure ??c). Finally, at $x_1 = 5\pi/2 - \theta/2 - \alpha/2$ until $x_1 = 3\pi/2$, the width of the profile is again $2r \sin \alpha/2$ (Figure ??d) and the size of α again limits the width of the profile.

The profile width p for π radians of rotation (from directly towards the sensor to directly behind the sensor) is completely characterised by the three intervals (Figure ??b–d). Average profile width \bar{p} is calculated by integrating these profiles over their appropriate intervals of x_1 and dividing by π which gives

$$\bar{p} = \frac{1}{\pi} \left(\int_{\frac{\pi}{2}}^{\frac{\pi}{2} + \frac{\theta}{2} - \frac{\alpha}{2}} 2r \sin \frac{\alpha}{2} dx_1 + \int_{\frac{\pi}{2} + \frac{\theta}{2} - \frac{\alpha}{2}}^{\frac{5\pi}{2} - \frac{\theta}{2} - \frac{\alpha}{2}} r \sin \frac{\alpha}{2} + r \cos \left(x_1 - \frac{\theta}{2} \right) dx_1 + \int_{\frac{5\pi}{2} - \frac{\theta}{2} - \frac{\alpha}{2}}^{\frac{3\pi}{2}} 2r \sin \frac{\alpha}{2} dx_1 \right) \quad \text{eqn 1}$$

$$= \frac{r}{\pi} \left(\theta \sin \frac{\alpha}{2} - \cos \frac{\alpha}{2} + \cos \left(\frac{\alpha}{2} + \theta \right) \right) \quad \text{eqn 2}$$

We then use this expression to calculate density

$$D = z/vt\bar{p}. \quad \text{eqn 3}$$

Rather than having one equation that describes \bar{p} globally, the gREM must be split into submodels due to discontinuous changes in p as α and β change. These discontinuities can occur for a number of reasons such as a profile switching between being limited by α and θ , the difference between very small profiles and profiles of size zero and the fact that the width of a sector stops increasing once the central angle reaches π radians (i.e., a semi circle is just as wide as a full circle.)

As a visual example, if α is small, there is an interval between Figure ??c and ??d where the ‘blind spot’ would prevent animals being detected at all giving $p = 0$. This would require an extra integral in our equation as simply putting our small value of α into eqn 1 would not give us this integral of $p = 0$.

gREM submodel specifications were done by hand, and the integration was done using SymPy (SymPy Development Team, 2014) in Python (Appendix S3). The gREM submodels were checked by confirming that: (1) submodels adjacent in parameter space were equal at the boundary between them; (2) submodels that border $\alpha = 0$ had $p = 0$ when $\alpha = 0$; (3) average profile widths \bar{p} were between 0 and $2r$ and; (4) each integral, divided by the range of angles that it was integrated over, was between 0 and $2r$. The scripts for these tests are included in Appendix S3 and the R (R Development Core Team, 2010) implementation of the gREM is given in Appendix S4.

Simulation Model. We tested the accuracy and precision of the gREM by developing a spatially explicit simulation of the interaction of sensors and animals using different combinations of sensor detection widths, animal signal widths, number of captures, and models of animal movement. 100 simulations were run where each consisted of a 7.5 km by 7.5 km square with periodic boundaries. A stationary sensor of radius r was set up in the exact centre of each simulation, covering 7 sensor detection widths θ between 0 and 2π ($2/9\pi, 4/9\pi, 6/9\pi, 8/9\pi, 10/9\pi, 14/9\pi, 2\pi$). Each simulation was populated with a density of 70 animals km^{-2} , calculated from the equation in Damuth (1981) as the expected density of mammals of weighing 1 g. This density therefore represents a reasonable estimate of density of individuals, given that the smallest mammal is around 2 g (Jones *et al.*, 2009). A total of 3937 individuals per simulation were created which were placed randomly at the start of the simulation. Individuals were assigned 11 signal widths α between 0 and π ($1/11\pi, 2/11\pi, 3/11\pi, 4/11\pi, 5/11\pi, 6/11\pi, 7/11\pi, 8/11\pi, 9/11\pi, 10/11\pi, \pi$).

Each simulation lasted for N steps (14400) of duration T (15 minutes) giving a total duration of 150 days. The individuals moved within each step with a distance d , with an average speed, v . d , was sampled from a normal distribution with mean distance, $\mu_d = vT$, and standard deviation $\sigma_d = vT/10$. An average speed, $v = 40 \text{ km day}^{-1}$, was chosen as this is the largest day range of terrestrial animals (Carbone *et al.*, 2005), and represents the upper limit of realistic speeds. At the end step, individuals were allowed to either remain stationary for a time step (with a

given probability, S), or change direction (in a uniform distribution with a maximum angle, A) between 0 and π . This resulted in 7 different movement models where: (1) simple movement, where S and $A = 0$; (2) stop-start movement, where (i) $S = 0.25$, $A = 0$, (ii) $S = 0.5$, $A = 0$, (iii) $S = 0.75$, $A = 0$; (3) random walk movement, where (i) $S = 0$, $A = \pi/3$, (ii) $S = 0$, $A = 2\pi/3$, (iii) $S = 0$, $A = \pi$. Individuals were counted as they moved in and out of the detection zone of the sensor per simulation.

We calculated the estimated animal density from the gREM by summing the number of captures per simulation and inputting these values into the correct gREM submodel. gREM accuracy was determined by comparing the density in the simulation with the estimated density. High accuracy is indicated by the mean difference between the estimated and actual values not being significantly different from zero (Wilcoxon signed-rank test). gREM precision was determined by the standard deviation of estimated densities. We used this method to compare the accuracy and precision of all the gREM submodels. As these submodels are derived for different combinations of α and θ , the accuracy and precision of the submodels was used to determine the impact of different values of α and θ .

The influence of the number of captures and animal movement models on accuracy and precision was investigated using 4 different gREM submodels representative of the range α and θ values (submodels NW1, SW1, NE1, and SE3, Figure 2). Using these four submodels, we calculated how long the simulation needed to run to generate a range of different capture numbers (from 10 to 100 captures in 10 unit intervals), and estimated animal density. These estimated densities were compared to the real density to assess the impact on the accuracy and precision of the gREM. The gREM assumes that individuals move continuously with straight-line movement (simple movement model) and we therefore assessed the impact of breaking the gREM assumptions. We used the four submodels to compare the accuracy and precision of a simple movement model, stop-start movement models and random walk movement models.

RESULTS

Analytical model. The equation for \bar{p} has been newly derived for each submodel in the gREM, except for the gas model and REM which have been calculated previously. However, many models, although derived separately, have the same expression for \bar{p} . Figure 4 shows the expression for \bar{p} in each case. The general equation for density, using the correct expression for \bar{p} is then substituted into eqn 3. Although more thorough checks are performed in Appendix S3, it can be seen that all adjacent expressions in Figure 4 are equal when expressions for the boundaries between them are substituted in.

Simulation model.

gREM submodels. All gREM submodels showed a high accuracy, i.e., the mean difference between the estimated and actual values was not significantly different from zero across all models, corrected for multiple tests (all gREM sub models Wilcoxon signed-rank test, $p > 0.002$)(Figure 5). However, the precision of the submodels do vary, where the gas model is the most precise and the SW7 sub model the least precise, having the smallest and the largest interquartile range, respectively (Figure 5). The standard deviation of the error between the estimated and true densities is strongly related to both the sensor and signal widths (Figure 6), such that larger widths have lower standard deviations (greater precision).

Number of captures. Within the four gREM submodels tested (NW1, SW1, SE3, NE1), the accuracy was not affected by the number of captures, where the mean difference between the estimated and actual values was not significantly different from zero across all capture rates, corrected for multiple tests (all gREM sub models Wilcoxon signed-rank test, $p > 0.008$)(Figure 7). However, the precision was dependent on the number of captures across all four of the gREM submodels, where precision increases as number of captures increases (Figure 7). For all gREM submodels, the the coefficient of variation falls to 10% at 100 captures.

Movement models. Within the four gREM submodels tested (NW1, SW1, SE3, NE1), neither the accuracy or precision was affected by the amount of time spent stationary. The mean difference between the estimated and actual values was not

significantly different from zero for each category of stationary time (0, 0.25, 0.5 and 0.75), corrected for multiple tests (all gREM sub models Wilcoxon signed-rank test, $p > 0.12$)(Figure 8a). Altering the maximum change in direction in each step (0, $\pi/3$, $2\pi/3$, and π) did not affect the accuracy or precision of the four gREM submodels tested (all gREM sub models Wilcoxon signed-rank test, $p > 0.05$)(Figure 8b).

DISCUSSION

We have developed the gREM such that it can be used to estimate density from acoustic sensors and camera traps. This has entailed a generalisation of the model and the REM in Rowcliffe *et al.* (2008) to be applicable to any combination of sensor width and signal directionality. We have used simulations to show, as a proof of principle, that these models are accurate and precise. The precision of the gREM was found to be dependent on the width of the sensor and the call, and the number of captures.

Analytical model. The gREM was derived for different combinations of α and θ resulting in 25 different submodels, the expression for \bar{p} are equal for many of these submodels resulting in eight different equations including the previously derived gas model and REM. These submodels were tested for consistency with adjacent expressions being equal at their boundaries. These new submodels will allow researchers to evaluate the absolute density of animals that have previously been difficult to study, such as bats (Clement & Castleberry, 2013), with noninvasive methods such as remote sensors. The gREM allows the data from acoustic detectors to be used where an animal has a directional calls, this could be used for a range of animals including songbirds (Blumstein *et al.*, 2011), and dolphins (Lammers & Au, 2003).

There are a number of possible extensions to the gREM which could be developed in the future. The original gas model was formulated for the case where both subjects, either animal and detector, or animal and animal, are moving (Hutchinson & Waser, 2007). Indeed any of the models with animals that are equally detectable in all directions ($\alpha = 2\pi$) can be trivially expanded for moving by substituting the sum of the average animal velocity and the sensor velocity for v as used

here. However, when the animal has a directional call, as seen in both terrestrial and aquatic environments (Lammers & Au, 2003; Blumstein *et al.*, 2011), the extension becomes less simple. The approach would be to calculate again the mean profile width. However, for each angle of approach, one would have to average the profile width for an animal facing in any direction (i.e. not necessarily moving towards the sensor) weighted by the relative velocity of that direction. There are a number of situations where a moving detector and animal could occur, e.g. an acoustic detector towed from a boat when studying porpoises (Kimura *et al.*, 2014) or surveying bats from a moving car (Ahlen & Baagøe, 1999; ?).

An interesting but unstudied problem is edge effects caused by trigger delays (the delay between sensing an animal and attempting to record the encounter) (Rovero *et al.*, 2013) and time expansion acoustic detectors which repeatedly turn on an off during sampling (Ahlen & Baagøe, 1999). Both of these have potential biases as animals can move through the detection zone without being detected. The models herein are formulated assuming constant surveillance and so the error created by switching the sensor on and off quickly becomes negligible if the sensor is on for extended periods of time. For example, if it takes longer for the recording device to be switched on than the length of some animal calls there could be a systematic underestimation of density.

Accuracy and Precision. Based on our simulations we believe that the gREM has the potential to produce accurate estimates for many different species, using either camera traps or acoustic detectors. However the precision of the gREM differed between submodels. For example, when the sensor and signal width were smaller than the precision of the model was reduced, so when choosing a sensor for use in a gREM study the detection width should be maximised, and if the study species has a narrow signal directionality other aspects of the study protocol, such as length of the survey, should be used to compensate.

The precision of the gREM is greatly affected by the number of captures that are collected, the coefficient of variation falls dramatically between 10 and 60 captures and then after this continues to slowly reduce. At 100 captures the submodels reach 10% coefficient of variation, considered to a very good level of precision

(Thomas & Marques, 2012). Many current studies do not reach this level of precision, with most studies reporting coefficient of variations greater than the 10% level (O'Brien *et al.*, 2003; Proctor *et al.*, 2010; Foster & Harmsen, 2012). The length of surveys in the field will need to be adjusted so that enough data can be collected to reach this level of precision. Populations of fast moving animals or populations with large densities will require less survey effort than those with slow moving or low densities.

The gREM was both accurate and precise for all the movement models we tested (stop-start movement and correlated random walks). However these movement models are still simple representations of true animal movement which are dependent on multiple factors such as behavioural state and existence of home ranges (Smouse *et al.*, 2010). The accuracy of the gREM may be affected by the interaction between the movement model and the size of the detection radius. We have studied a relatively long step length compared to the size of the detection radius, and therefore the chance of catching the same animal multiple times within a short space of time was reduced and there is little effect on the precision of the model (Figure 8b). However if the ratio of step length to detection radius was smaller then this may decrease the precision of the model, however this should not decrease its accuracy.

Although we have used simulations to validate the gREM submodels, much more robust testing is needed. Although difficult, proper field test validation would be required before the models could be fully trusted. The REM (Rowcliffe *et al.*, 2008) has already been field tested, and both Rowcliffe *et al.* (2008) and Zero *et al.* (2013) both found that the REM was an effective manner of estimating animal densities (Rowcliffe *et al.*, 2008; Zero *et al.*, 2013). In some taxa gold standard methods of estimating animal density exist, such as capture mark recapture (Sollmann *et al.*, 2013). Where these gold standard exist or true numbers are known, a simultaneous gREM study could be completed to test the accuracy under field conditions, similar to the tests that Rowcliffe *et al.* (2008) completed with the REM. An easier way to continue to evaluate the models is to run more extensive simulations which break the assumptions of the analytical models. The main element that

cannot be analytically treated is the complex movement of real animals. Therefore testing these methods against true animal traces, or more complex movement models would be required.

Within the simulation we have assumed an equal density across the entire world, however in a field environment the situation would be much more complex, with additional variation coming from local changes in density between camera sites. We allowed the sensor to be stationary and on all the time, negating the triggering, and time expansion issues that could exist in real life. In the simulation we ran the speed of the animal as 40 km day⁻¹, the largest day range of terrestrial animals (Carbone *et al.*, 2005). Other speed values should not alter the accuracy of the gREM (precision would be affected, all else being equal, since slower speeds produce fewer records). We also assume perfect knowledge of the average speed of an animal and size of the detection zone, and instant triggering of the camera. All of which may lead to possible bias or a decrease in precision.

Implications for conservation. The gREM is available for the estimation of density of a number of taxa where no, or few, accurate methods currently exist to measure absolute animal density (Thomas & Marques, 2012). The species that can now be studied may be of importance to conservation, for example current methods of density estimation for the threatened Franciscana dolphin may result in underestimation of numbers (Crespo *et al.*, 2010). This new method may be important for the study of zoonotic diseases, for example estimating population sizes of bats, which are important reservoir of infectious disease that affect humans, livestock and wildlife (Calisher *et al.*, 2006). In addition, the gREM will make it possible to measure the density of animals which may be useful in quantifying ecosystem services, such as studying the levels of songbirds which are known to have a positive influence on pest control in coffee production (Jirinec *et al.*, 2011). The gREM is suitable for any species that would be consistently recorded within range of a detector, such as bats (Kunz *et al.*, 2009), songbirds (Buckland & Handel, 2006), whales (Marques *et al.*, 2009) or forest primates (Hassel-Finnegan *et al.*, 2008). With increasing technological capabilities, this list of species is likely to increase dramatically.

Importantly the camera trapping and acoustic recording that the gREM use are noninvasive and do not require individual marking (Jewell, 2013) or naturally identifying marks (as required for mark-recapture models). This makes them suitable for large, continuous monitoring projects with limited human resources (Kelly *et al.*, 2012). It also makes them suitable for species that are under pressure, species that cannot naturally be individually recognised or species that are difficult or dangerous to catch (Thomas & Marques, 2012).

1. ACKNOWLEDGMENTS

REFERENCES

- Acevedo, M.A. & Villanueva-Rivera, L.J. (2006) Using automated digital recording systems as effective tools for the monitoring of birds and amphibians. *Wildlife Society Bulletin*, **34**, 211–214.
- Ahlen, I. & Baagøe, H.J. (1999) Use of ultrasound detectors for bat studies in europe: experiences from field identification, surveys, and monitoring. *Acta Chiropterologica*, **1**, 137–150.
- Anderson, D.R. (2001) The need to get the basics right in wildlife field studies. *Wildlife Society Bulletin*, pp. 1294–1297.
- Barlow, J. & Taylor, B. (2005) Estimates of sperm whale abundance in the northeastern temperate pacific from a combined acoustic and visual survey. *Marine Mammal Science*, **21**, 429–445.
- Blumstein, D.T., Mennill, D.J., Clemins, P., Girod, L., Yao, K., Patricelli, G., Deppe, J.L., Krakauer, A.H., Clark, C., Cortopassi, K.A. *et al.* (2011) Acoustic monitoring in terrestrial environments using microphone arrays: applications, technological considerations and prospectus. *Journal of Applied Ecology*, **48**, 758–767.
- Borchers, D., Distiller, G., Foster, R., Harmsen, B. & Milazzo, L. (2014) Continuous-time spatially explicit capture–recapture models, with an application to a jaguar camera-trap survey. *Methods in Ecology and Evolution*.
- Brusa, A. & Bunker, D.E. (2014) Increasing the precision of canopy closure estimates from hemispherical photography: Blue channel analysis and under-exposure. *Agricultural and Forest Meteorology*, **195**, 102–107.

- 456 Buckland, S.T. & Handel, C. (2006) Point-transect surveys for songbirds: robust
457 methodologies. *The Auk*, **123**, 345–357.
- 458 Buckland, S.T., Marsden, S.J. & Green, R.E. (2008) Estimating bird abundance:
459 making methods work. *Bird Conservation International*, **18**, S91–S108.
- 460 Calisher, C., Childs, J., Field, H., Holmes, K. & Schountz, T. (2006) Bats: important
461 reservoir hosts of emerging viruses. *Clinical microbiology reviews*, **19**, 531–545.
- 462 Carbone, C., Cowlshaw, G., Isaac, N.J. & Rowcliffe, J.M. (2005) How far do ani-
463 mals go? Determinants of day range in mammals. *The American Naturalist*, **165**,
464 290–297.
- 465 Clark, C.W. (1995) Application of US Navy underwater hydrophone arrays for
466 scientific research on whales. *Reports of the International Whaling Commission*, **45**,
467 210–212.
- 468 Clement, M.J. & Castleberry, S.B. (2013) Estimating density of a forest-dwelling
469 bat: a predictive model for rafinesque’s big-eared bat. *Population Ecology*, **55**,
470 205–215.
- 471 Crespo, E.A., Pedraza, S.N., Grandi, M.F., Dans, S.L. & Garaffo, G.V. (2010) Abun-
472 dance and distribution of endangered franciscana dolphins in argentine waters
473 and conservation implications. *Marine Mammal Science*, **26**, 17–35.
- 474 Cutler, T.L. & Swann, D.E. (1999) Using remote photography in wildlife ecology:
475 a review. *Wildlife Society Bulletin*, pp. 571–581.
- 476 Damuth, J. (1981) Population density and body size in mammals. *Nature*, **290**,
477 699–700.
- 478 Depraetere, M., Pavoine, S., Jiguet, F., Gasc, A., Duvail, S. & Sueur, J. (2012) Mon-
479 itoring animal diversity using acoustic indices: implementation in a temperate
480 woodland. *Ecological Indicators*, **13**, 46–54.
- 481 Elphick, C.S. (2008) How you count counts: the importance of methods research
482 in applied ecology. *Journal of Applied Ecology*, **45**, 1313–1320.
- 483 Everatt, K.T., Andresen, L. & Somers, M.J. (2014) Trophic scaling and occupancy
484 analysis reveals a lion population limited by top-down anthropogenic pressure
485 in the limpopo national park, mozambique. *PloS one*, **9**, e99389.
- 486 Foster, R.J. & Harmsen, B.J. (2012) A critique of density estimation from camera-
487 trap data. *The Journal of Wildlife Management*, **76**, 224–236.

- 488 Harris, D., Matias, L., Thomas, L., Harwood, J. & Geissler, W.H. (2013) Applying
489 distance sampling to fin whale calls recorded by single seismic instruments in
490 the northeast atlantic. *The Journal of the Acoustical Society of America*, **134**, 3522–
491 3535.
- 492 Hassel-Finnegan, H.M., Borries, C., Larney, E., Umponjan, M. & Koenig, A. (2008)
493 How reliable are density estimates for diurnal primates? *International Journal of*
494 *Primatology*, **29**, 1175–1187.
- 495 Hayes, J.P. (2000) Assumptions and practical considerations in the design and in-
496 terpretation of echolocation-monitoring studies. *Acta Chiropterologica*, **2**, 225–
497 236.
- 498 Hutchinson, J.M.C. & Waser, P.M. (2007) Use, misuse and extensions of “ideal gas”
499 models of animal encounter. *Biological Reviews of the Cambridge Philosophical So-*
500 *ciet*y, **82**, 335–359.
- 501 Jewell, Z. (2013) Effect of monitoring technique on quality of conservation science.
502 *Conservation Biology*, **27**, 501–508.
- 503 Jirinec, V., Campos, B.R. & Johnson, M.D. (2011) Roosting behaviour of a migratory
504 songbird on jamaican coffee farms: landscape composition may affect delivery
505 of an ecosystem service. *Bird Conservation International*, **21**, 353–361.
- 506 Jones, K.E., Bielby, J., Cardillo, M., Fritz, S.A., O'Dell, J., Orme, C.D.L., Safi, K.,
507 Sechrest, W., Boakes, E.H., Carbone, C. *et al.* (2009) PanTHERIA: a species-level
508 database of life history, ecology, and geography of extant and recently extinct
509 mammals: Ecological archives e090-184. *Ecology*, **90**, 2648–2648.
- 510 Jones, K.E., Russ, J.A., Bashta, A.T., Bilhari, Z., Catto, C., Csősz, I., Gorbachev,
511 A., Győrfi, P., Hughes, A., Ivashkiv, I. *et al.* (2011) Indicator bats program: a
512 system for the global acoustic monitoring of bats. *Biodiversity Monitoring and*
513 *Conservation: Bridging the Gap between Global Commitment and Local Action*, pp.
514 211–247.
- 515 Karanth, K. (1995) Estimating tiger (*Panthera tigris*) populations from camera-trap
516 data using capture–recapture models. *Biological Conservation*, **71**, 333–338.
- 517 Kelly, M.J., Betsch, J., Wultsch, C., Mesa, B. & Mills, L.S. (2012) Noninvasive sam-
518 pling for carnivores. *Carnivore ecology and conservation: a handbook of techniques*
519 (*L Boitani and RA Powell, eds*) Oxford University Press, New York, pp. 47–69.

- 520 Kessel, S., Cooke, S., Heupel, M., Hussey, N., Simpfendorfer, C., Vagle, S. & Fisk, A.
521 (2014) A review of detection range testing in aquatic passive acoustic telemetry
522 studies. *Reviews in Fish Biology and Fisheries*, **24**, 199–218.
- 523 Kimura, S., Akamatsu, T., Dong, L., Wang, K., Wang, D., Shibata, Y. & Arai, N.
524 (2014) Acoustic capture-recapture method for towed acoustic surveys of echolo-
525 cating porpoises. *The Journal of the Acoustical Society of America*, **135**, 3364–3370.
- 526 Kunz, T.H., Betke, M., Hristov, N.I. & Vonhof, M. (2009) Methods for assessing
527 colony size, population size, and relative abundance of bats. *Ecological and be-*
528 *havioral methods for the study of bats (TH Kunz and S Parsons, eds) 2nd ed Johns*
529 *Hopkins University Press, Baltimore, Maryland*, pp. 133–157.
- 530 Lammers, M.O. & Au, W.W. (2003) Directionality in the whistles of hawaiian spin-
531 ner dolphins (*stenella longirostris*): A signal feature to cue direction of move-
532 ment? *Marine Mammal Science*, **19**, 249–264.
- 533 Lewis, T., Gillespie, D., Lacey, C., Matthews, J., Danbolt, M., Leaper, R.,
534 McLanaghan, R. & Moscrop, A. (2007) Sperm whale abundance estimates from
535 acoustic surveys of the ionian sea and straits of sicily in 2003. *Journal of the Ma-*
536 *rine Biological Association of the United Kingdom*, **87**, 353–357.
- 537 Manzo, E., Bartolommei, P., Rowcliffe, J.M. & Cozzolino, R. (2012) Estimation of
538 population density of european pine marten in central italy using camera trap-
539 ping. *Acta Theriologica*, **57**, 165–172.
- 540 Marcoux, M., Auger-Méthé, M., Chmelnitsky, E.G., Ferguson, S.H. & Humphries,
541 M.M. (2011) Local passive acoustic monitoring of narwhal presence in the cana-
542 dian arctic: a pilot project. *Arctic*, pp. 307–316.
- 543 Marques, T.A., Munger, L., Thomas, L., Wiggins, S. & Hildebrand, J.A. (2011) Es-
544 timating North Pacific right whale (*Eubalaena japonica*) density using passive
545 acoustic cue counting. *Endangered Species Research*, **13**, 163–172.
- 546 Marques, T.A., Thomas, L., Ward, J., DiMarzio, N. & Tyack, P.L. (2009) Estimating
547 cetacean population density using fixed passive acoustic sensors: An example
548 with Blainville’s beaked whales. *The Journal of the Acoustical Society of America*,
549 **125**, 1982–1994.
- 550 O’Brien, T.G., Kinnaird, M.F. & Wibisono, H.T. (2003) Crouching tigers, hidden
551 prey: Sumatran tiger and prey populations in a tropical forest landscape. *Animal*

- 552 *Conservation*, **6**, 131–139.
- 553 O'Farrell, M.J. & Gannon, W.L. (1999) A comparison of acoustic versus capture
554 techniques for the inventory of bats. *Journal of Mammalogy*, pp. 24–30.
- 555 Proctor, M., McLellan, B., Boulanger, J., Apps, C., Stenhouse, G., Paetkau, D. &
556 Mowat, G. (2010) Ecological investigations of grizzly bears in Canada using DNA
557 from hair, 1995–2005: a review of methods and progress. *Ursus*, **21**, 169–188.
- 558 Purvis, A., Gittleman, J.L., Cowlishaw, G. & Mace, G.M. (2000) Predicting extinc-
559 tion risk in declining species. *Proceedings of the Royal Society of London Series B:*
560 *Biological Sciences*, **267**, 1947–1952.
- 561 R Development Core Team (2010) *R: A Language And Environment For Statistical*
562 *Computing*. R Foundation For Statistical Computing, Vienna, Austria. ISBN 3-
563 900051-07-0.
- 564 Richter-Dyn, N. & Goel, N.S. (1972) On the extinction of a colonizing species. *The-*
565 *oretical Population Biology*, **3**, 406–433.
- 566 Rogers, T.L., Ciaglia, M.B., Klinck, H. & Southwell, C. (2013) Density can be mis-
567 leading for low-density species: benefits of passive acoustic monitoring. *Public*
568 *Library of Science One*, **8**, e52542.
- 569 Rovero, F., Zimmermann, F., Berzi, D. & Meek, P. (2013) "which camera trap type
570 and how many do I need?" a review of camera features and study designs for a
571 range of wildlife research applications. *Hystrix*.
- 572 Rowcliffe, J.M. & Carbone, C. (2008) Surveys using camera traps: are we looking
573 to a brighter future? *Animal Conservation*, **11**, 185–186.
- 574 Rowcliffe, J., Field, J., Turvey, S. & Carbone, C. (2008) Estimating animal density
575 using camera traps without the need for individual recognition. *Journal of Ap-*
576 *plied Ecology*, **45**, 1228–1236.
- 577 Schmidt, B.R. (2003) Count data, detection probabilities, and the demography, dy-
578 namics, distribution, and decline of amphibians. *Comptes Rendus Biologies*, **326**,
579 119–124.
- 580 Smouse, P.E., Focardi, S., Moorcroft, P.R., Kie, J.G., Forester, J.D. & Morales, J.M.
581 (2010) Stochastic modelling of animal movement. *Philosophical Transactions of the*
582 *Royal Society B: Biological Sciences*, **365**, 2201–2211.

- 583 Soisalo, M.K. & Cavalcanti, S. (2006) Estimating the density of a jaguar population
584 in the Brazilian Pantanal using camera-traps and capture-recapture sampling in
585 combination with GPS radio-telemetry. *Biological Conservation*, **129**, 487–496.
- 586 Sollmann, R., Gardner, B., Chandler, R.B., Shindle, D.B., Onorato, D.P., Royle, J.A.
587 & O’Connell, A.F. (2013) Using multiple data sources provides density estimates
588 for endangered florida panther. *Journal of Applied Ecology*, **50**, 961–968.
- 589 SymPy Development Team (2014) *SymPy: Python library for symbolic mathematics*.
- 590 Thomas, L. & Marques, T.A. (2012) Passive acoustic monitoring for estimating an-
591 imal density. *Acoustics Today*, **8**, 35–44.
- 592 Trolle, M. & Kéry, M. (2003) Estimation of ocelot density in the Pantanal using
593 capture-recapture analysis of camera-trapping data. *Journal of mammalogy*, **84**,
594 607–614.
- 595 Trolle, M., Noss, A.J., Lima, E.D.S. & Dalponte, J.C. (2007) Camera-trap studies of
596 maned wolf density in the Cerrado and the Pantanal of Brazil. *Biodiversity and
597 Conservation*, **16**, 1197–1204.
- 598 Walters, C.L., Collen, A., Lucas, T.C.D., Mroz, K., Sayer, C.A. & Jones, K.E. (2013)
599 Challenges of using bioacoustics to globally monitor bats. *Bat Evolution, Ecology,
600 and Conservation*, pp. 479–499. Springer.
- 601 Wright, S.J. & Hubbell, S.P. (1983) Stochastic extinction and reserve size: a focal
602 species approach. *Oikos*, pp. 466–476.
- 603 Yapp, W. (1956) The theory of line transects. *Bird study*, **3**, 93–104.
- 604 Zero, V.H., Sundaresan, S.R., O’Brien, T.G. & Kinnaïrd, M.F. (2013) Monitoring
605 an endangered savannah ungulate, Grevy’s zebra (*Equus grevyi*): choosing a
606 method for estimating population densities. *Oryx*, **47**, 410–419.

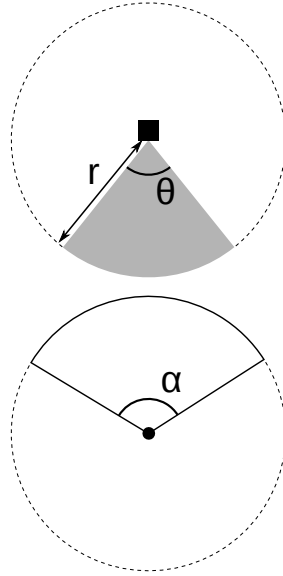


FIGURE 1. Representation of sensor detection width and animal signal width. The filled square and circle represent a sensor and an animal, respectively; θ , sensor detection width (radians); r , sensor detection distance; dark grey shaded area, sensor detection zone; α , animal signal width (radians). Dashed lines around the filled square and circle represents the maximum extent of θ and α , respectively.

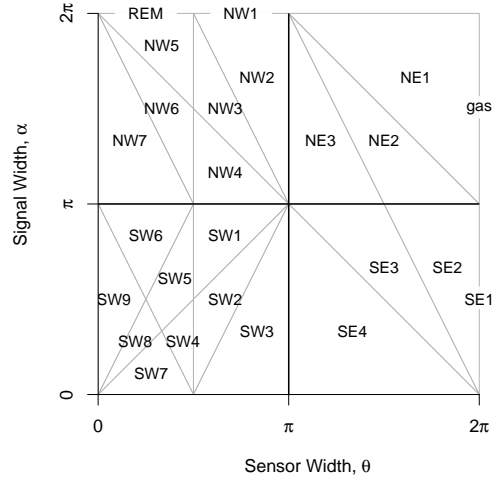


FIGURE 2. Locations where derivation of the average profile \bar{p} is the same for different combinations of sensor detection width and animal signal width. Symbols within each polygon refer to each gREM submodel named after their compass point, except for Gas and REM which highlight the position of these previously derived models within the gREM. Symbols on the edge of the plot are for submodels with $\alpha, \theta = 2\pi$

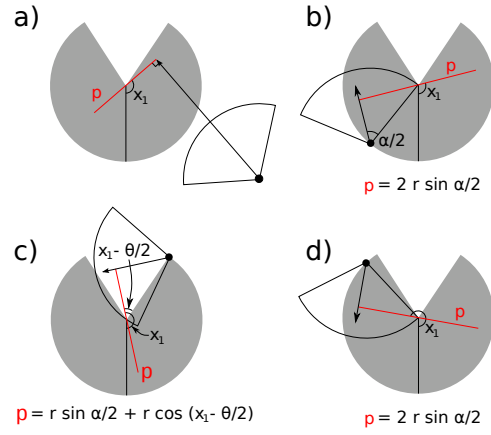


FIGURE 3. An overview of the derivation of SE2. The filled circles represent animals, with the animal signal shown as an unfilled sector and the direction of movement shown as an arrow. The detection zone of the sensor is shown as filled grey sectors with a detection distance of r . The vertical black line within the circle shows the direction the sensor is facing; θ , sensor detection width; α , animal signal width. The profile p (the line an animal must pass through in order to be captured) is shown in red and x_1 is the focal angle, where (a) shows the location of x_1 . The derivation of p changes as the animal approaches the sensor from different directions where (b) is the derivation of p when x_1 is in the interval $[\frac{\pi}{2}, \frac{\pi}{2} + \frac{\theta}{2} - \frac{\alpha}{2}]$, (c) p when x_1 is in the interval $[\frac{\pi}{2} + \frac{\theta}{2} - \frac{\alpha}{2}, \frac{5\pi}{2} - \frac{\theta}{2} - \frac{\alpha}{2}]$ and (d) p when x_1 is in the interval $[\frac{5\pi}{2} - \frac{\theta}{2} - \frac{\alpha}{2}, \frac{3\pi}{2}]$. The resultant equation for p is shown beneath each figure.

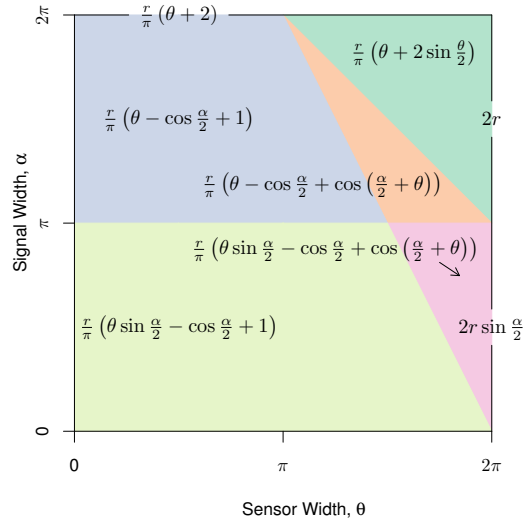


FIGURE 4. Expressions for the average profile width, \bar{p} , given sensor and signal widths. Despite independent derivation within each block, many models result in the same expression. These are collected together and presented as one block of colour. Expressions on the edge of the plot are for submodels with $\alpha, \theta = 2\pi$.

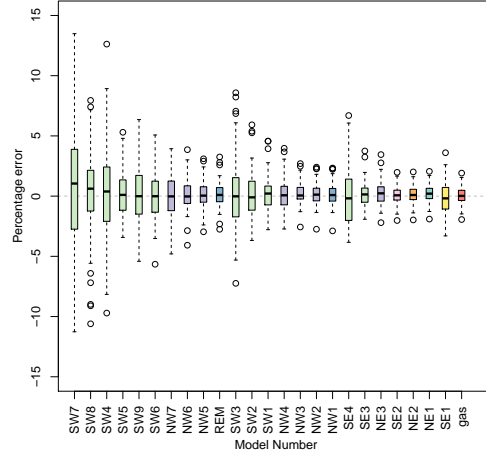


FIGURE 5. Simulation model results of the accuracy and precision for gREM submodels. The percentage error between estimated and true density for each gREM submodel is shown within each box plot, where the black line represents the median percentage error across all simulations, boxes represent the the middle 50% of the data, whiskers represent variability outside the upper and lower quartiles with outliers plotted as individual points. Box colours correspond to the expressions for average profile width \bar{p} given in Figure 4.

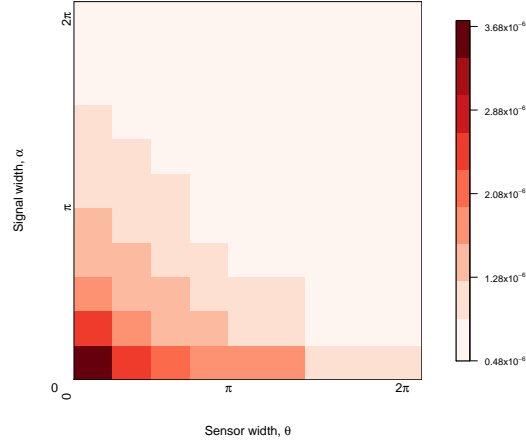


FIGURE 6. Simulation model results of the gREM precision given a range of sensor and signal widths, shown by the standard deviation of the error between the estimated and true densities. Standard deviations are shown from deep red to pink, representing high to low values between 0.483×10^{-6} to 3.74×10^{-6} .

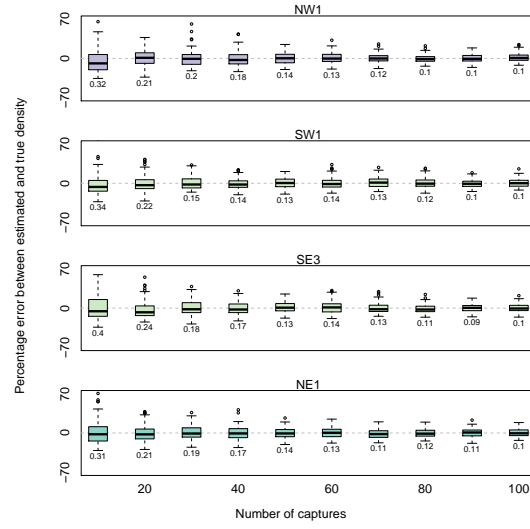


FIGURE 7. Simulation model results of the accuracy and precision of four gREM submodels (NW1, SW1, SE3 and NE1) given different numbers of captures. The percentage error between estimated and true density within each gREM sub model for capture rate is shown within each box plot. Sensor and signal widths vary between submodels. The number beneath each plot represents the coefficient of variation. The colour of each box plot corresponds to the expressions for average profile width \bar{p} given in Figure 4.

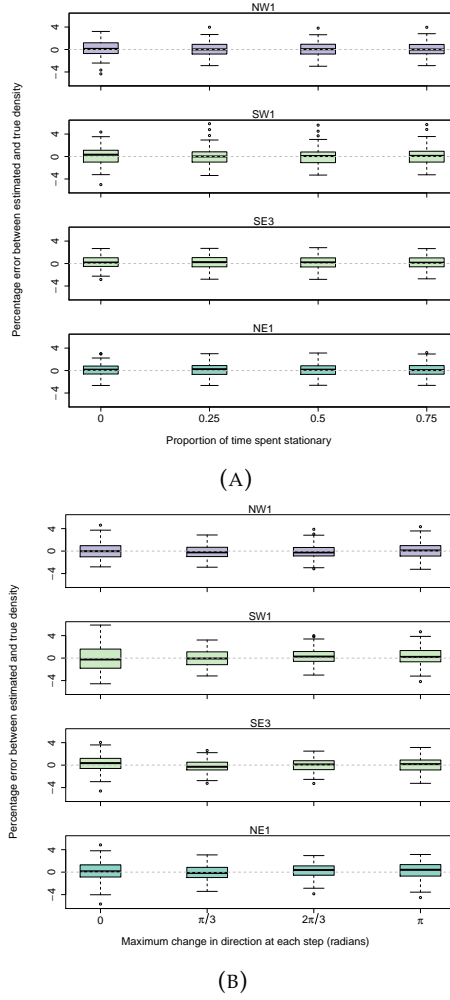


FIGURE 8. Simulation model results of the accuracy and precision of four gREM submodels (NW1, SW1, SE3 and NE1) given different movement models where (A) amount of time spent stationary (stop-start movement) and (B) maximum change in direction at each step (correlated random walk model). The percentage error between estimated and true density within each gREM sub model for the different movement models is shown within each box plot. The simple model is represented where time and maximum change in direction equals 0. The colour of each box plot corresponds to the expressions for average profile width \bar{p} given in Figure 4.